Distribution Agreement

In presenting this thesis as a partial fulfillment of the requirements for a degree from Emory University, I hereby grant to Emory University and its agents the non-exclusive license to archive, make accessible, and display my thesis in whole or in part in all forms of media, now or hereafter now, including display on the World Wide Web. I understand that I may select some access restrictions as part of the online submission of this thesis. I retain all ownership rights to the copyright of the thesis. I also retain the right to use in future works (such as articles or books) all or part of this thesis.

Sol Lee March 22, 2017

Differential expression of vesicular glutamate transporter 2 in thalamostriatal terminals

by

Sol Lee

Yoland Smith, PhD

Adviser

Department of Neuroscience and Behavioral Biology

Yoland Smith, PhD

Adviser

Leah Roesch, PhD

Committee Member

Randy Hall, PhD

Committee Member

2017

Differential expression of vesicular glutamate transporter 2 in thalamostriatal terminals

By

Sol Lee

Yoland Smith, PhD

Adviser

An abstract of
a thesis submitted to the Faculty of Emory College of Arts and Sciences
of Emory University in partial fulfillment of the requirements of the degree of
Bachelor of Sciences with Honors

Department of Neuroscience and Behavioral Biology

2017

Abstract

Differential expression of vesicular glutamate transporter 2
in thalamostriatal terminals

by Sol Lee

Glutamate is the main excitatory neurotransmitter in the central nervous system, and its transmission is crucial for regulating cognitive functions such as learning and memory. Glutamate transporters help maintain the homeostasis of the glutamatergic system, and vesicular glutamate transporter 2 (vGluT2) in particular is known to be a marker of thalamostriatal projections in the brain. It is unclear, however, as to whether or not the striatum expresses vGluT2-positive as well as vGluT2-negative thalamostriatal projections. This study sought to better understand the expression of vGlut2 in the thalamostriatal system. The anterograde axonal tracer Phaseolus vulgaris-leucoagglutinin (PHA-L) was used to trace projections in 10 adult Sprague Dawley rats from the central medial (CeM) and the parafascicular (Pf) nuclei of the thalamus to the striatum, and immunogold labeling was also used to localize vGluT2 in the striatal tissue. After double-labeling, the striatal tissue was processed and examined with electron microscopy and confocal light microscopy. Anterogradely-labeled terminals from the CeM and the Pf were categorized as PHA-L/vGluT2-positive or PHA-L/vGluT2-negative, and the proportion of vGluT2-immunoreactivity from the CeM and the Pf was quantified to better understand the expression of vGluT2 in the thalamostriatal system. An average of 39.3% (± 4.98%) from the CeM and 47.0% (± 7.55%) from the Pf of the anterogradely-labeled thalamostriatal terminals expressed no vGluT2-immunoreactivity at the EM level. At the confocal microscopic level, an average of 86.7% (± 1.61%) from the CeM and 72.6% (± 3.84%) of the terminals from the Pf were vGluT2-negative. These results suggest that there is a subpopulation of thalamostriatal neurons that do not express vGluT2 and that the thalamostriatal system may give rise to both vGluT2-positive and vGluT2-negative terminals.

Differential expression of vesicular glutamate transporter 2 in thalamostriatal terminals

By

Sol Lee

Yoland Smith, PhD

Adviser

A thesis submitted to the Faculty of Emory College of Arts and Sciences
of Emory University in partial fulfillment
of the requirements of the degree of
Bachelor of Sciences with Honors

Department of Neuroscience and Behavioral Biology

2017

Acknowledgements

I would like to thank Dr. Yoland Smith for his tremendous support and guidance throughout my time in his laboratory. I would like to thank Jeff Paré and Susan Jenkins for their care in teaching and explaining the necessary skills required to complete this study.

Table of Contents

Differential expression of vesicular glutamate transporter 2 in thalamostriatal terminals

by Sol Lee

Yerkes National Primate Research Center

Honors Thesis

INTRODUCTION

History of vGluTs

Glutamate has been known as the predominant excitatory neurotransmitter in the central nervous system since 1984 (Fonnum, 1984), but the mechanism behind its transport into synaptic vesicles was unknown for many years. In 1994, a protein that was able to transport inorganic phosphate was discovered, and due to its properties, it was named brain-specific Na^+-dependent inorganic phosphate co-transporter, or BNPI (Ni et al., 1994). Later, it was discovered that BNPI was localized in presynaptic terminals and preferentially associated with synaptic vesicular membranes (Bellocchio et al., 1998) and that mutations in the BNPI homologue in *C. elegans* caused decreases in glutamatergic transmission (Lee et al., 1999). Two independent papers also corroborated the role of BNPI in glutamatergic transport, and so BNPI was more appropriately renamed vesicular glutamate transporter, or vGluT.

Shortly after, a protein that shares 82% amino acid homology with vGluT (thereafter named vGluT1) was identified, and this newly-discovered protein also demonstrated a similar role in vesicular glutamate transport (Fujiama et al., 2001; Sakata-Haga et al., 2001). This protein, named vGluT2, became the second of three proteins in the vesicular glutamate transporter family. The last member vGluT3 was identified when researchers studied numerous

dopaminergic and serotonergic neurons that released glutamate, but failed to express vGluT1 or vGluT2 (Gras et al., 2002).

All three members of the vGluT family are greatly homologous, sharing nearly 90% homology with one another, but the N- and C-terminals of the three vGluTs have little homology. All three vGluTs also share similar transport properties (Bellocchio et al., 2000; Fremeau et al., 2001; Takamori et al., 2000) and are dependent on a proton gradient that is created by hydrolyzing adenosine triphosphate (ATP) with V-type H^+-ATPase. This provides a flow of positively-charged hydrogen ions into the synaptic vesicles and makes them more acidic, generating a pH gradient. As the interior of the vesicle becomes more positive, an electrochemical proton gradient is also generated.

With regards to differences between the vGluTs, there are well-documented differences between the regional distributions of the three vGluTs. vGluT3 is the most distinct member of the vGluT family as it is less common in the central nervous system (CNS) and does not co-localize with other vGluT isoforms (Boulland et al., 2004). vGluT3 is also localized in a limited and particular set of neurons in the neocortex, hippocampus, olfactory bulb, hypothalamus, substantia nigra, and raphe nuclei (Fremeau et al., 2002; Gras et al., 2002; Herzog et al., 2004). The distribution of vGluT3 is broad, but restricted to specific neuronal populations. Most notably, vGluT3 is the only member of its family that is expressed in the dendrites of striatal neurons (Fremeau et al., 2002), and it usually co-localizes with markers of neurons that do not primarily express glutamate.

The other two vGluTs, vGluT1 and vGluT2, are mainly associated with glutamatergic neurons. Their expression in the CNS is complementary, and there is little overlap with each other; vGluT1 is found in layers I-III of the neocortex, the piriform and piriform cortex, the

amygdala, and the hippocampus, while vGluT2 is present in layer IV of the cerebral cortex, the olfactory bulb, the thalamus, the hypothalamus, and the brainstem (Fremeau et al., 2001; Herzog et al., 2001; Kaneko et al., 2002). Because of differences in their regional distributions, scientists have attempted to functionally characterize vGluT1 and vGluT2. It has been suggested that vGluT1 is expressed at synapses that exhibit long-term potentiation (LTP) and low glutamate release probability, while vGluT2 is expressed in synapses with long-term depression (LTD) and high release probability (Fremeau et al., 2001; Varoqui et al., 2002). Co-expression does occur in the brain - vGluT1 and vGluT2 are both expressed in the hippocampus (Herzog et al., 1998), neocortex (Nakamura et al., 2005), spinal cord (Persson et al., 2006), and cerebellum (Boulland et al., 2004) – but co-expression of vGluT1 and vGluT2 in a few areas remains the exception to the normally complementary pattern of vGluT1 and vGluT2 in the adult brain.

The Dual Thalamostriatal System

The striatum and subthalamic nucleus serve as the main 'entry doors' to the basal ganglia, which receives glutamatergic input from the thalamus and cerebral cortex. The thalamostriatal and corticostriatal systems have distinctive properties, but glutamate and its transporters are heavily implicated in both systems. In discussing the thalamostriatal system, however, it is meaningful to distinguish the centromedian and parafascicular complex (CM/Pf) of the thalamus apart from the rest of the thalamic nuclei. Most thalamic nuclei send projections to the striatum, but the CM/Pf complex (mainly represented by the Pf in rodents) is the main source of thalamic input to the striatum in both primates and non-primates (Sadikot et al., 1992; Smith et al., 2004; Raju et al., 2006). Although the CM/Pf complex provides minor input to the cerebral cortex and massive projections to the striatum, the non-CM/Pf thalamic nuclei are more

cortically than striatally directed. In the striatum, the cellular targets and synaptic connectivity of the CM/Pf and the non-CM/Pf nuclei differ in that CM/Pf afferents contact both medium spiny neurons (MSN) and interneurons (IN), forming mostly asymmetric axo-dendritic synapses, while the principal targets of non-CM/Pf thalamostriatal projections are MSNs, forming almost exclusively axo-spinous synapses. The CM/Pf nuclei, for unknown reasons, also undergo severe early degeneration in Parkinson's Disease (PD), while the non-CM/Pf nuclei are not affected in PD.

It is important to note that vGluT1 is primarily expressed in glutamatergic neurons from the cerebral cortex and that vGluT2 is primarily expressed in glutamatergic neurons from the thalamus, so much so that vGluT1 is considered to be a marker for corticostriatal projections and vGluT2 for thalamostriatal projections (Hur and Zaborszky, 2005; Raju & Smith, 2006; Raju et al., 2008; Figure 1). Although this is the case, it is unknown as to whether or not vGluT1 and vGluT2 are absolute markers of all corticostriatal and thalamostriatal projections, respectively. Incidentally, a study conducted by Raju *et al.* in 2008 reported that about 20% of putative glutamatergic terminals in the striatum did not express vGluT1 or vGluT2, suggesting the expression of another vGluTs in a subset of striatal glutamatergic terminals. To investigate this issue further, this study utilized anterograde axonal tract tracing methods, along with confocal microscopy and electron microscopy, to quantify the percentage of anterogradely-labeled terminals from the central medial (CeM) and the Pf thalamic nuclei to the rat striatum that express or not vGluT2. The CeM and the Pf were chosen as two representative thalamic nuclei because of the different properties of the CM/Pf versus the non-CM/Pf nuclei in the dual thalamostriatal system (Smith et al., 2014).

The purpose of this study was to determine whether or not there is a subpopulation of thalamic glutamatergic terminals in the adult rat striatum that do not express vGluT2. The present study hypothesized that there would be a significant percentage of thalamostriatal terminals from the CeM and the Pf that do not express vGluT2. If there was a proportion of anterogradely-labeled terminals that did not express vGluT2, it would support the hypothesis and suggest that the thalamus gives rise to both vGluT2-positive and vGluT2-negative thalamostriatal projections. On the other hand, if all anterogradely-labeled CeM and Pf terminals were vGluT2-positive, it would indicate that another extrinsic source (most likely not from the cerebral cortex) gives rise to vGluT1-negative terminals in the striatum. The present study hypothesized that the subpopulation of striatal terminals that did not express any of the known vGluTs would be thalamic in origin and that, accordingly, vGluT2 would not be an absolute marker for all thalamostriatal projections.

Prior research has suggested that vGluTs are involved in Parkinson's Disease (Lievens et al., 2001), as well as Alzheimer's Disease (Masliah, 2000), Huntington's Disease (Behrens et al., 2002), cerebral stroke (Maragakis and Rothstein, 2004), and epilepsy (Sepkuty et al., 2002), and findings from this study may also help to elucidate whether or not vGluT2 is an absolute marker of all putative glutamatergic terminals from the thalamus, which is important because there is significant loss and dysfunction of glutamatergic terminals in the striatum of Parkinsonian animal models. A deeper understanding of the exact sources of the different types of glutamatergic terminals in the mammalian striatum is essential to assess the functional significance of this glutamatergic network pathology in Parkinson's disease and to better understand the neural pathways and role of vGluTs in the brain.

MATERIALS AND METHODS

Animals and tissue preparation

A total of 10 adult Sprague Dawley rats were used in this study. The animals were housed and cared for in the Yerkes Primate Center rodent vivarium. The care and experimental conditions used in this study followed the *Guide for the Care and Use of Laboratory Animals* by the National Institute of Health and were approved by the Institutional Animal Care and Use Committee of Emory University.

The axonal anterograde tracer Phaseolus vulgaris-leucoagglutinin (PHA-L) was used to trace projections from the CeM and the Pf to the striatum. The tracer was delivered in the CeM and the Pf of rats through intracerebral surgeries as described previously (Unal et al., 2014). Ten days after the injection, animals were deeply euthanized and sacrificed by fixative perfusion with an overdose of pentobarbital (100 mg/kg) and perfused transcardially with cold oxygenated Ringer's solution, followed by 2 liters of fixative containing 4% paraformaldehyde and 0.1% glutaraldehyde in phosphate buffer (PB; 0.1 M, pH 7.4). After perfusion, the brains were washed with phosphate buffer, removed from the skull, and then processed to localize PHA-L and vGluT2 on striatal tissue.

Immunoperoxidase labeling for electron microscopy

Striatal tissue sections (60 μm thick) from 10 adult rats were sectioned with a vibratome, collected in cold phosphate-buffered saline (PBS; 0.01 M, pH 7.5), and treated with sodium borohydride (1% in PBS) for 20 minutes. After thoroughly rinsing the the sections in PBS, they were placed in a cryoprotectant solution (PB; 0.05 m, pH 7.4, containing 25% sucrose and 10%

glycerol) for 20 min, frozen at -80 °C for 20 min, thawed, and returned to a graded series of cryoprotectant (100, 70, 50 and 30%) diluted in PBS.

The tissue sections were pre-incubated in 5% milk solution in PBS for 30 minutes, then rinsed 3 x 5 minutes in TBS-gelatin buffer. The sections were then incubated overnight at room temperature with the antisera diluted at 1/2000 for rabbit anti-PHA-L and guinea pig-antivGluT2 at 1/5000 in TBS-gelatin buffer. The next morning, the sections were thoroughly rinsed 3 x 10 minutes in TBS-gelatin and transferred to a secondary antibody solution containing goat anti-rabbit biotinylated (1/200) to label PHA-L, and goat anti-guinea pig coupled with gold particles (1/100) to label vGluT2 in gold. The sections were incubated for 2 hours at room temperature, and then rinsed 2 x 10 minutes in TBS-gelatin and once for 10 minutes in acetate buffer (2% aqueous solution, pH 7.0). Silver enhancement of gold particles was then done using HQ silver kit. After being rinsed rinsed 3 x 10 minutes in acetate buffer and 1 x 10 minutes in TBS-gelatin, the tissue sections were then incubated in a solution containing 1% avidin-biotin complex diluted in TBS-gelatin with 1% milk at room temperature for 90 minutes. The sections were then rinsed 2 x 10 minutes in TBS-gelatin and 1 x 10 min in Tris-buffered saline (TBS).

The sections were preincubated in a solution containing 10% normal goat serum and 1% bovine serum albumin in PBS for 1 hour. They were then incubated for 48 hours at 4 deg C° with the antisera diluted at 0.2 μg/ml in a solution containing 1% normal goat serum (NGS) and 1% bovine serum albumin (BSA) in PBS. Next, the sections were rinsed in PBS and transferred for 1.5 hours to a secondary antibody solution containing biotinylated goat anti- rabbit IgGs, diluted 1:200. After rinsing, sections were put in a solution containing 1% avidin-biotin-peroxidase complex (Vector). The tissue was then washed in PBS and Tris buffer (0.05 M pH 7.6) before being transferred into a solution containing 0.01 M-imidazole, 0.005% hydrogen

peroxide, and 0.025% 3,30-diaminobenzidine tetrahydrochloride (DAB) in Tris for 10 minutes. The DAB reaction was terminated with several rinses in PBS.

Following the immunostaining reactions, the sections were transferred to PB (0.1 M, pH 7.4) for 10 minutes and exposed to 1% osmium tetroxide for 20 minutes. They were then rinsed with PB and dehydrated in an increasing gradient of ethanol. Uranyl acetate (1%) was added to the 70% alcohol step in the gradient in order to increase contrast at the EM. The sections were then treated with propylene oxide before being embedded in epoxy resin for 12 hours, mounted on microscope slides, and placed in a 60 C° oven for 48 hours.

Sections were then processed for EM and ultrathin sections were cut and collected on single slot copper grids as previously described (Galvan et al., 2006; Gonzales et al., 2013). As a control for the specificity of the immunolabeling, omission of the primary antibody from the incubation solution virtually abolished the immunostaining. The EM was used to visualize anterogradely labeled terminals from the CeM and the Pf nuclei in the striatum. This method was combined with the immunogold method to localize vGluT2 with specific antibodies. The tissue was prepared for EM and analyzed with a JEOLL model 1011 transmission electron microscope.

Data were collected exclusively from sections on the surface of the blocks to ensure optimal antibody penetration into the tissue. Series of 50 random electron micrographs of PHA-L- labeled terminals (from areas where both the peroxidase and immunogold markers could be seen in close vicinity) were taken at 25,000x. Only structures that could be clearly identified were quantified.

A negative control experiment was also conducted using 2 animals; PHA-L tracers were injected into the CeM of one adult rat and into the Pf of the other. The procedures followed similarly as listed above except for the immunogold labeling of vGluT1 instead of vGluT2.

Immunofluorescent staining for light microscopy

Tissue sections from the precommissural and postcommissural striatal levels in rat brains were used to quantify the area of striatum occupied by vGluT2 immunofluorescence. After the striatal tissue sections were cut on the vibratome (60 μm), they were collected in cold PBS (0.01 M, pH 7.5) and treated with sodium borohydride (1% in PBS) for 20 minutes. The sections were preincubated in a solution containing 5% normal donkey serum, 1% BSA, and 0.3% Triton X-100 in PBS for an hour. After rinsing 3 x 5 minutes in PBS, the sections were placed with the primary antisera in an incubation solution diluted at 1/2000 for rabbit anti-PHA-L and guinea pig-anti-vGluT2 at 1/5000 in PBS. 1% normal donkey serum and 1% BSA were added, and the solution was incubated overnight at room temperature.

The next morning, the sections were rinsed 3 x 10 minutes in PBS, then transferred to a secondary antibody solution containing donkey anti-rabbit coupled with Rhodamine Red-X, donkey anti-guinea pig coupled with fluorescein isothiocyanate, 1% normal donkey serum, and 1% BSA for 2 hours at room temperature. The sections were rinsed for 3 x 10 minutes in PBS, and then placed in cupric sulfate solution for 30 mins at room temperature. The sections were rinsed 3 x 10 minutes in PBS, and then mounted with Vectashield and stored at 4 °C. Sections were scanned with a confocal microscope, and final images were prepared using Image J.

Analysis of material

Electron microscopic material

Striatal tissue from 5 adult rats with anterogradely-labeled tracers in the CeM and tissue from 3 adult rats with tracers in the Pf were used for EM. To minimize false negatives, ultrathin sections from the most superficial sections of blocks were scanned at 25,000x, and ultrathin

sections were randomly scanned for the presence of immunoreactive terminals only when gold particles were also visible in the same field of view. These boutons were photographed and categorized as either PHA-L/vGluT2-positive or PHA-L/vGluT2-negative. To reduce false negatives, boutons that were labeled as PHA-L/vGluT2-positive were required to have 3 or more gold particles co-localized with the PHA-L tracer (Figure 2). The relative proportions were calculated and then expressed as the mean percentage (± SEM) of total anterogradely-labeled axon terminals (labeled with peroxidase deposit) coming from the thalamus (either the CeM or the Pf). Student's unpaired t-test was used to assess statistical differences between vGluT2-immunoreactivity in the CeM versus in the Pf, and the 1-sample z-test was used to assess the statistical difference between co-localized and non-co-localized PHA-L terminals from the CeM nucleus and then in the Pf nucleus. These thalamic nuclei were chosen to represent the CM/Pf complex and the non-CM/Pf nuclei in the dual thalamostriatal system.

Confocal Microscopy Material

A second series of experiments was also performed using the confocal microscope instead of the EM. Using Image J, confocal light microscopic images were adjusted for contrast and brightness. PHA-L, localized with fluorescein isothiocyanate, was visualized in green, and vGluT2, localized with Rhodamine Red-X, was visualized in red. The proportion of thalamostriatal vGluT2-immunoreactive varicosities were quantified by adjusting images for contrast and brightness in order to differentiate co-localized (PHA-L/vGluT-positive) terminals from single-labeled (PHA-L/vGluT2-negative) terminals. Co-localized terminal-like varicosities appeared yellow (Figure 3). Similarly to the way done at the EM level, striatal terminal-like varicosities from the CeM and the Pf were categorized either PHA-L/vGluT2-positive or PHA-

L/vGluT2-negative. Their relative proportions were also calculated and expressed as the mean percentage (± SEM), and an unpaired t-test and z-test were used to assess statistical differences between the same groups as described above.

RESULTS

PHA-L tracers were injected into the CeM and the Pf in the adult rat brain. Injection sites are visually represented in Figure 4. At the EM level, there was a significant proportion of labeled terminals that co-expressed PHA-L and vGluT2 after injections in either the CeM or Pf ($p < 0.05$; Figure 5). From the 273 thalamostriatal terminals that were sampled from the CeM nucleus, 39.3% (± 4.98%) of these thalamostriatal terminals were vGluT2-negative, and from the 293 terminals sampled from the Pf nucleus, 47.0% (± 7.55%) were vGluT2-negative. At the confocal microscopic level, there was also a significant proportion of PHA-L/vGluT2-negative terminals ($p < 0.05$; Figure 5). From the 467 PHA-L-containing terminal-like profiles from the CeM, 86.7% (± 1.61%) were vGluT2-negative, and from the 710 terminals sample from the Pf, 72.6% (± 3.84%) were vGluT2-negative.

Student's unpaired t-test was used to assess the statistical difference between PHA-L/vGluT2-positive and PHA-L/vGluT2-negative terminals from the CeM and the Pf. In assessing the statistical difference between the percentage of vGluT2-positive and vGluT2-negative thalamostriatal terminals for the CeM nucleus at the EM level, there was a statistically significant difference found ($p = 0.0041$). There was also a statistically significant difference between the percentage of vGluT2-positive and vGluT2-negative terminals for the Pf nucleus at

the EM level ($p = 0.0046$). An unpaired t-test also revealed no significant difference in vGluT2-immunoreactivity between the CeM and the Pf ($p = 0.2748$) at the EM level.

At the confocal microscopic level, the unpaired t-test revealed a statistically significant difference between PHA-L/vGluT2-positive and PHA-L/vGluT2-negative terminals in the CeM ($p = 0.0000$) and in the Pf ($p = 0.0000$). An unpaired t-test also found a statistically significant difference in vGluT2-immunoreactivity in the CeM and the Pf ($p = 0.0019$).

A negative control experiment examined the vGluT1-immunoreactivity of thalamostriatal projections from the CeM and the Pf. 53 terminals were examined from the CeM, and 61 from the Pf. No terminals were double-labeled (PHA-L/vGluT1-positive), and there was a significant difference found between vGluT1-immunoreactivity in the CeM versus in the Pf ($p = 0.045$).

DISCUSSION

Anterograde tracers were used in this study to determine if there was a proportion of thalamostriatal terminals that did not express vGluT2. Our findings, indeed, revealed that a significant percentage of vGluT2-negative terminals arose from both the CeM and the Pf, which were chosen to be representative of the dual thalamostriatal system. Additionally, there was no statistical difference between the proportion of vGluT2-positive and vGluT2-negative terminals that came from the either thalamic nuclei. These findings are the first of its kind to directly quantify the percentage of vGluT2-negative terminals that arise in the thalamostriatal system, and significant proportion of vGluT2-negative terminals that came from the CeM and the Pf reveal that there may be another vGluT expressed in these terminals. At the very least, these data reinforce the need to investigate this issue further.

This finding supports the original hypothesis that there would be a significant percentage of thalamostriatal terminals from the CeM and the Pf that do not express vGluT2. At the confocal microscopic level, there was also a significant proportion of PHA-L/vGluT2-negative terminals ($p < 0.05$; Figure 6), further suggesting that the thalamus gives rise to both vGluT2-positive and vGluT2-negative thalamostriatal projections. There was no significant difference in vGluT2-immunoreactivity between the CeM and the Pf at the EM level ($p < 0.05$, Figure 6), but there was a significant difference in vGluT2-immunoreactivity between the CeM and the Pf at the confocal microscopic level. This study purposely avoided the definitive labeling of the terminal-like varicosities as terminals because unlike at the EM level, it is difficult to definitively state whether the varicosities observed were terminals or another part of the neuron. This may explain the statistically significant finding at the confocal microscopic level; it is currently unknown as to what degree vGluT is expressed on different parts of the neuron. However, the relatively high p value ($p = 0.275$; Figure 5) at the EM level suggests that the projection of vGluT2-negative thalamostriatal terminals does not seem to be nuclei-specific.

The negative control experiment, which also used the double-labeling method, utilizing the PHA-L tracer in thalamic projections and immunogold labeling for the expression of vGluT, had no PHA-L/vGluT2-positive terminals. 53 terminals from the CeM and 61 terminals from the Pf were examined. This suggests that technical issues with labeling did not lead to false negatives in the actual experiment.

Technical considerations

These data, in line with the results from the study by Raju et al. in 2008, suggest the presence of another vGluT. Care was taken to minimize false negatives at several steps, but it is

still important to take caution in assuming the existence of another vGluT or a subset of an existing vGluT solely on the basis of negative data. In this study, false negatives were minimized by using sections from the most superficial sections of blocks. This was done because peroxidase is known to penetrate tissue more deeply than gold particles, and it would otherwise have been possible for the observer to be viewing regions where there is peroxidase, but no gold staining. Additionally, in order to ascertain the expression of vGluT2, boutons were labeled as PHA-L/vGluT2-positive only if they had 3 or more gold particles co-localized with the PHA-L tracer.

Previous research suggests that it is highly unlikely that the vGluT2-negative terminals coming from the CeM and the Pf express vGluT1 or vGluT3 because of differences in the regional distributions of vGluT1 and vGluT3. In particular, vGluT3 is expressed in primarily non-glutamatergic terminals. However, the absence of detectable vGluT2 immunoreactivity in these terminals does not necessarily mean that these terminals are completely devoid of vGluT2. The vGluT2 protein may not be expressed at a high enough level to be appropriately labeled with the antibody. Although the vGluT2 gene may be expressed, the amount of translated proteins may not reach levels high enough because of imbalance between synthesis and degradation of the vGlut2 protein. It is noteworthy that the level of mRNA expression does not always correlate to normal protein expression (Shyu et al., 2008).

The finding of vGluT2-negative terminals at both the EM and confocal microscopic levels help affirm that this may not be due to simply technical issues, but even the negative data in this study at the EM and confocal microscopic level were not very consistent; an average of 43.1% of thalamostriatal projections at the EM level and 79.6% of thalamostriatal projections at the confocal microscopic level were vGluT2-negative. This discrepancy may be explained by the different nature of labeling and observing at the EM versus the confocal level. At the EM level,

the observer is looking for axon terminals that express both PHA-L and gold particles, representing expression of vGluT2. At the confocal level, it is more difficult to discriminate between pre-terminals unmyelinated axons and axon terminals, and it is possible that vGluT2 is not expressed as highly in axons as it is in axon terminals. In this manner, it may have been possible that the number of negatives were higher at the confocal level because of the differential proportion of axons and axon terminals at the EM and confocal microscopic level.

Future directions

It would be possible to strengthen the results of this study by adding more animals and reevaluating the methods used to account for unforeseen technical issues that may explain the lack of vGluT2 in anterogradely-labeled terminals. A possible negative control that can be done to test the anterograde tracer PHA-L and immunogold labeling would be to use PHA-L to trace projections from the cortex to the striatum and to use immunogold labeling to localize vGluT2 in the striatal tissue. Because vGluT1 almost exclusively labels corticostriatal projections, it would be expected that this experiment would yield no PHA-L/vGluT2-positive corticostriatal terminals. Testing other thalamic nuclei would also help corroborate the results from this study as the CeM and the Pf were chosen to be representative regions of the dual thalamostriatal system. This will help determine if the lack of vGluT2 in thalamostriatal terminals is a feature that characterizes other thalamostriatal projections. The most direct and clear way to ensure the reduction of technical problems, however, may be to use 2 different antibodies for vGluT2 concurrently in a triple-labeling experiment. By doing so, it would become much clearer if there were to be a technical issue with one antibody or the other.

In the future, it would be important to study the proportion of thalamic terminals that

express vGluT2 in other brain regions such as the cerebral cortex or the amygdala to determine if the pattern of vGluT2 distribution seen in the striatum characterizes thalamic projections throughout the brain. Furthermore, it would be useful to study the postsynaptic targets of thalamostriatal projections. It is possible that these non-vGluT2 terminals may preferentially target a particular group of striatal neurons. Understanding this level of specificity and the synaptic properties of these terminals is important because in some diseased states, different regions of the nervous system may be targeted. Thus, less of particular regions would disproportionately affect expression of that vGluT. The present study suggested that there is a subpopulation of thalamostriatal neurons that do not express vGluT2 and that thalamostriatal system may give rise to both vGluT2-positive and vGluT2-negative terminals. Further studies to address this issue will allow us to better understand their function and integration within the complex synaptic network of the mammalian striatum.

CONCLUSION

The present study showed a significant percentage of anterogradely-labeled terminals from the Pf and the CeM that do not express vGluT2 in the rat striatum. This finding points to the possibility that the thalamus may give rise to both vGluT2-positive and vGluT2-negative thalamostriatal projections and suggests that this differentiation does not seem to be nuclei-specific. The findings of this study provide a greater understanding of the sources of the different types of glutamatergic terminals in the mammalian striatum and suggests that vGluT2 is not an absolute marker of all thalamostriatal terminals in rodents, but it is recommended that more research should be conducted, particularly in the form of a triple-labeling experiment, to reach a more conclusive outcome.

TABLES AND FIGURES

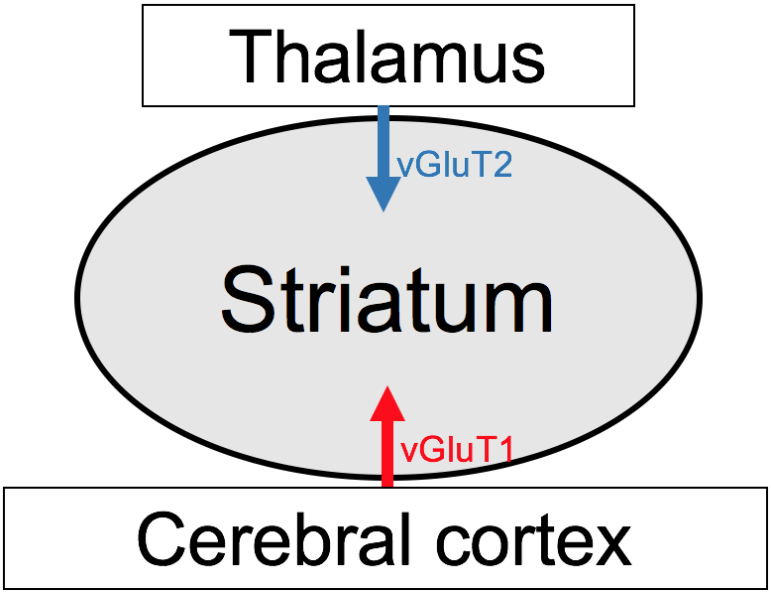

Figure 1. A simplified model of the thalamostriatal and corticostriatal pathways. vGluT1 is a marker for cortical projections to the striatum, while vGluT2 is a marker for thalamic projections to the striatum.

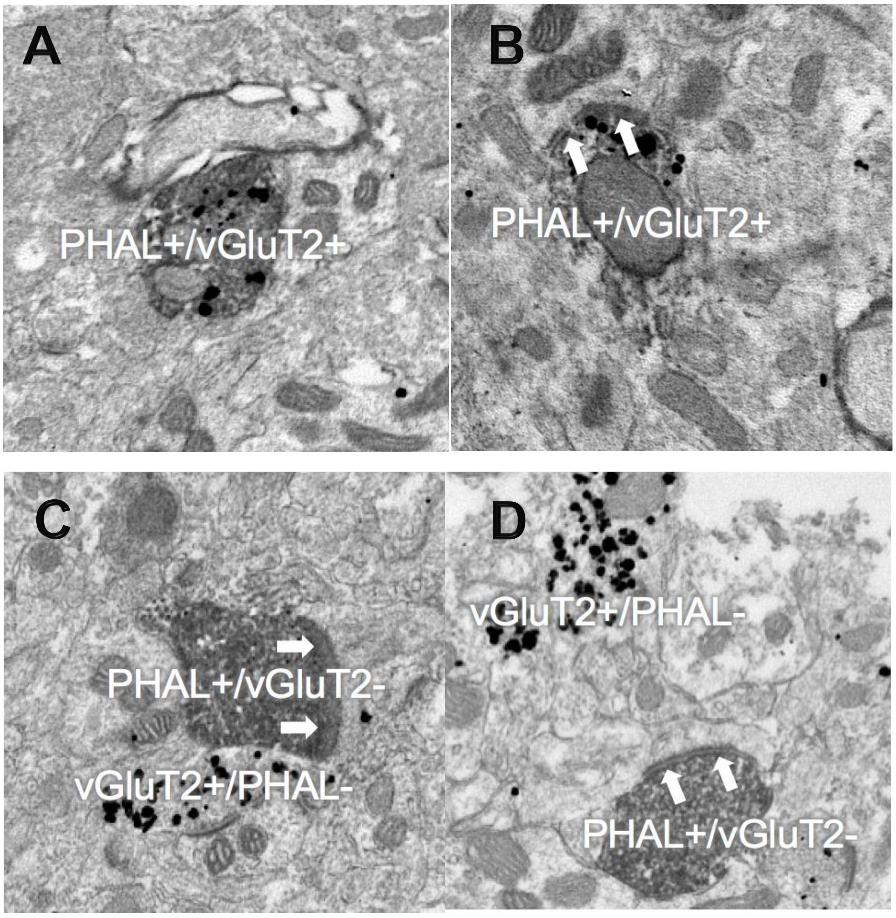

Figure 2. (A-D) Electron micrographs of PHA-L-containing (peroxidase) and vGluT2-immunolabeled (silver-intensified gold particles) terminals in the rat striatum. Labeled terminals in A and C are from the CeM, while labeled terminals in B and D are from the Pf. **A-B:** PHAL/vGluT2-positive terminals co-labeled for vGLuT2. **C-D:** PHA-L/vGluT2-positive terminals that do not express vGluT2. Single-labeled vGluT2-positive terminals (gold) are shown in close proximity to the anterogradely-labeled boutons. The white arrows indicate asymmetric synapses.

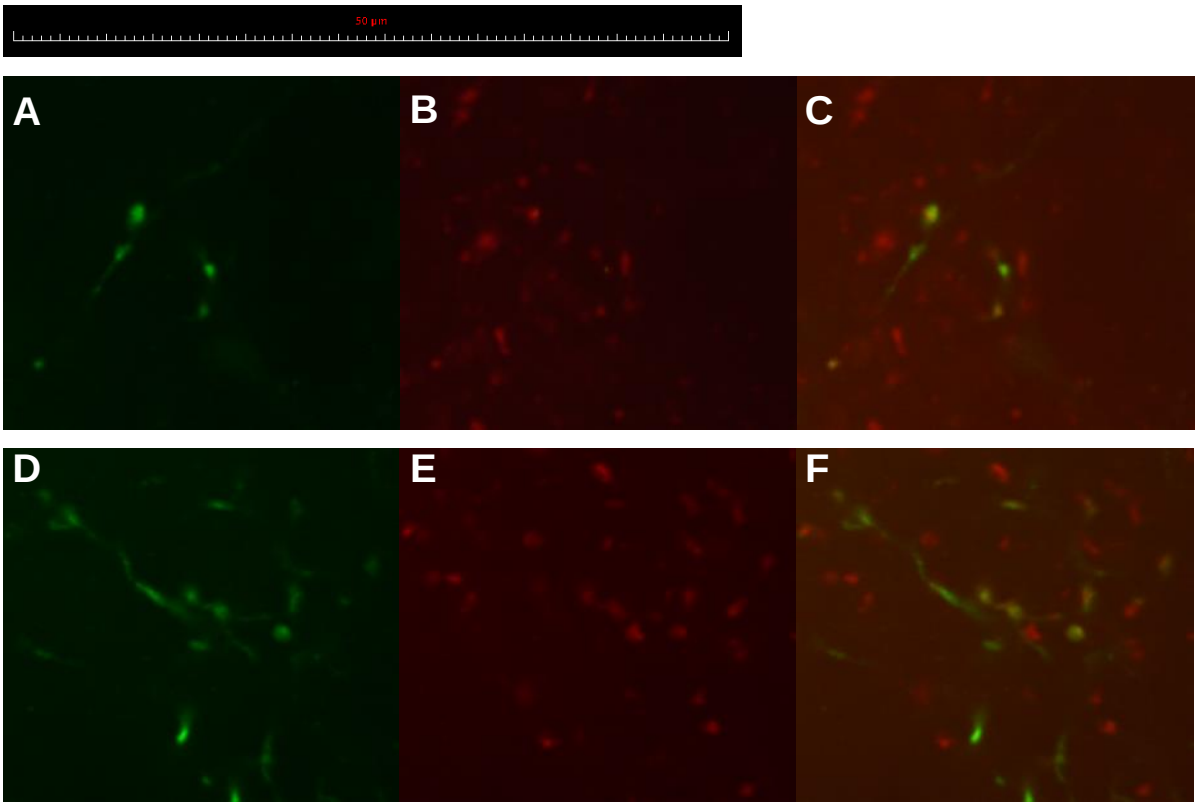

Figure 3. (A-F) Confocal light microscopic images visualized through ImageJ. Rhodamine Red-X was used to visualize expression of vGluT2 in red, and fluorescein isothiocyanate was used to visualize PHA-L in green. Image J was used to visualize confocal light microscopic images and adjust for contrast and brightness. **A-C:** Thalamostriatal tissue with PHA-L injections from the CeM. A was adjusted to visualize PHA-L. B was adjusted to visualize vGluT2. C was adjusted to see the co-localized (PHA-L/vGluT2-positive) terminal-like projections. **D-F:** Thalamostriatal tissue with PHA-L injections from the Pf.

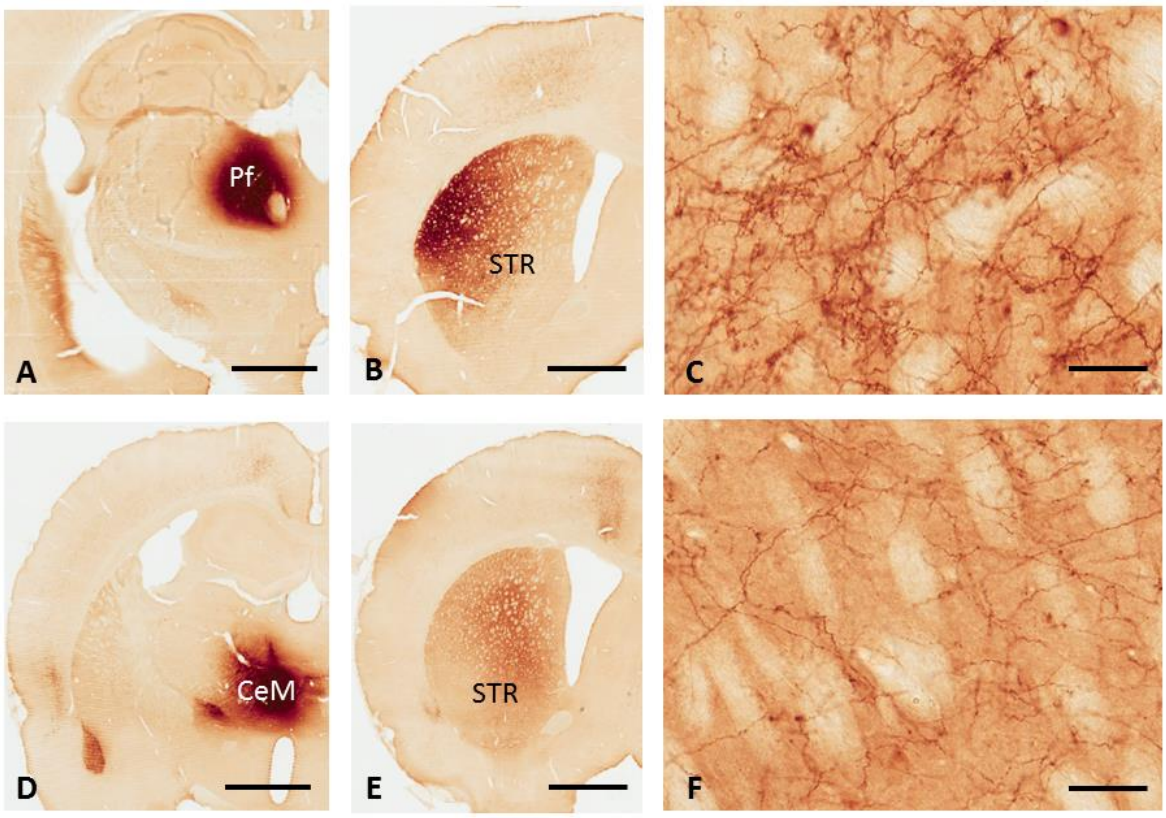

Figure 4: Light micrographs showing the PHA-L injection sites in the Pf (A) and CeM (D) thalamic nuclei. B and C illustrate low and high power views of resulting anterograde labeling of axonal and terminal profiles in the ipsilateral striatum after Pf injection. E and F illustrate PHA-L labeling in the striatum after CeM injection. Scale bars: A,B,D,E: 1 mm; C,F: 50 um.

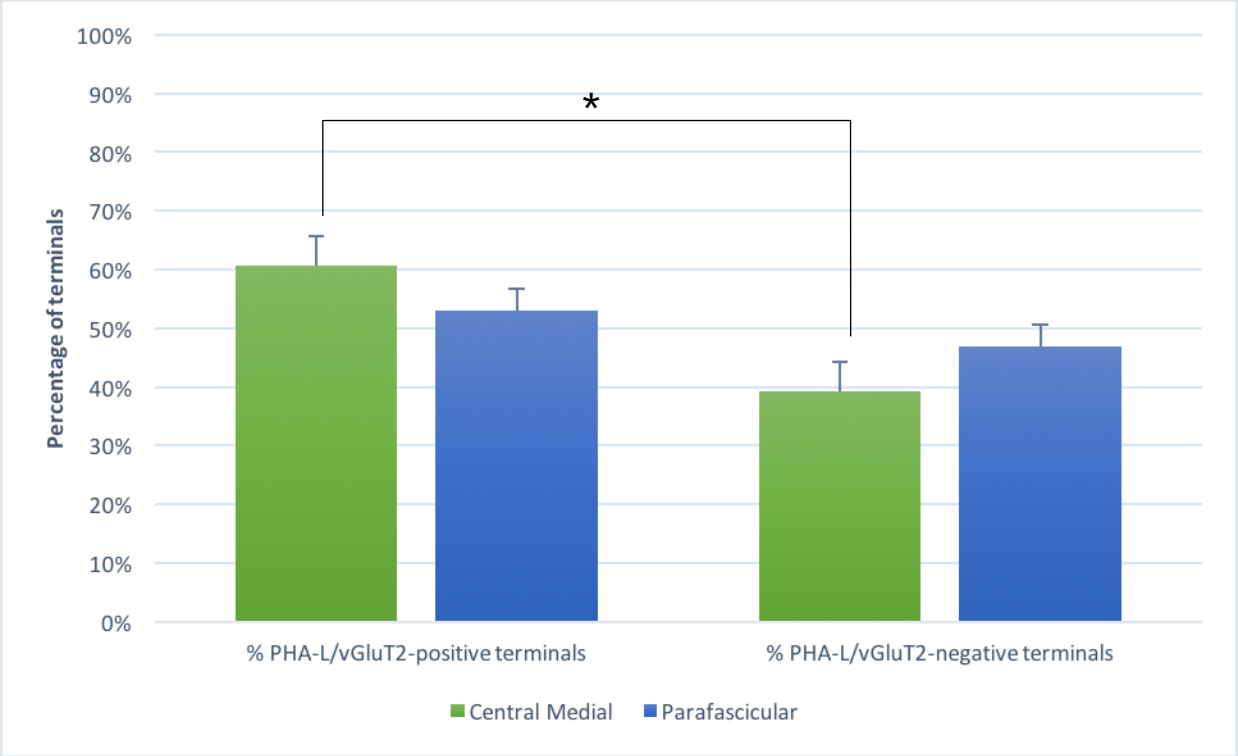

Figure 5. Quantitative analysis of the proportion of anterogradely-labeled terminals from the CeM and the Pf that express vGluT2-immunoreactivity in the rat striatum at the EM level. 273 anterogradely-labeled terminals from the CeM and 293 terminals from the Pf were sampled for this analysis. Error bars represent the standard error of the mean. An unpaired t-test revealed no significant difference in vGluT2-immunoreactivity between the CeM and the Pf ($p = 0.275$). The 1-sample z-test was used to find that there was a significant difference between PHA-L/vGluT2-positive and PHA-L/vGluT2-negative terminals in the CeM ($p = 0.0002$), but no significant difference between PHA-L/vGLuT2-positive and PHA-L/vGLuT2-negative terminals in the Pf ($p = 0.1865$). ($^*p < 0.05$)

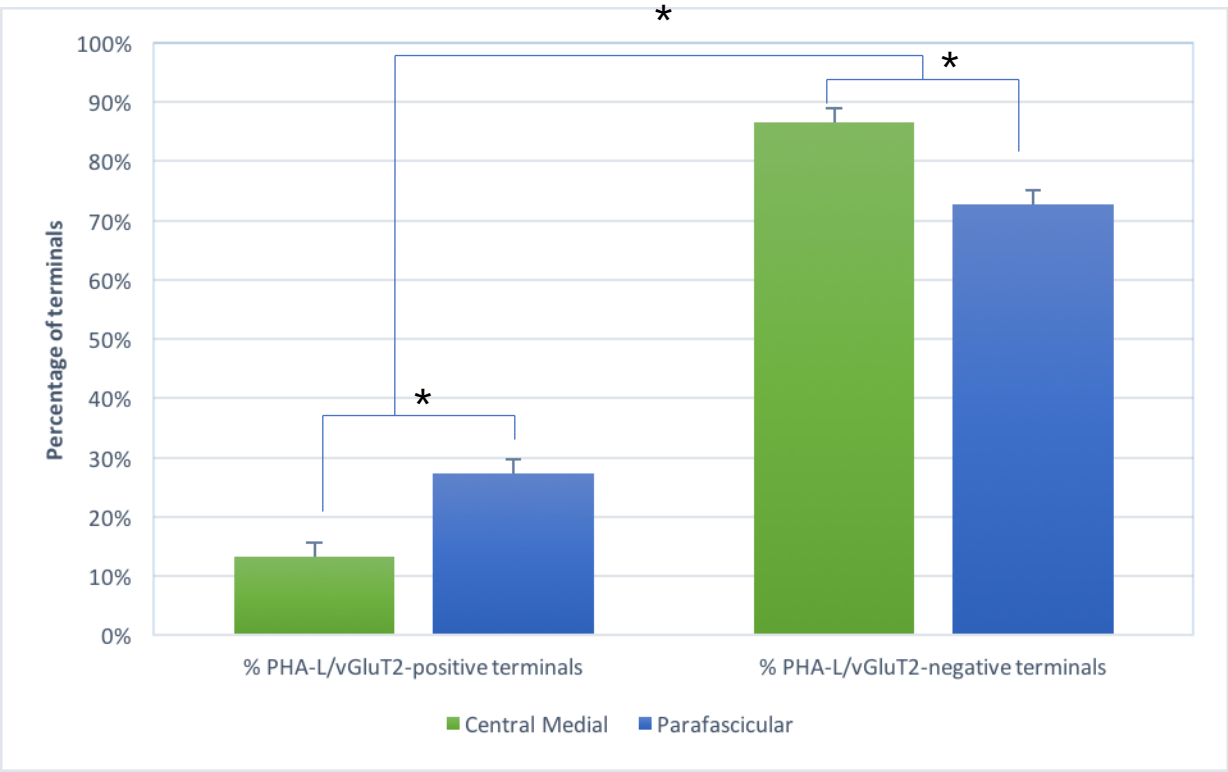

Figure 6. Quantitative analysis of the proportion of anterogradely-labeled terminals from the CeM and the Pf that express vGluT2-immunoreactivity in the rat striatum at the confocal microscopic level. 467 anterogradely-labeled terminals from the CeM and 710 terminals from the Pf were sampled for this analysis. Error bars represent the standard error of the mean. An unpaired t-test found a significant difference between vGluT2-immunoreactivity in the CeM and the Pf ($p = 0.001926$). 1-sample z-test also a significant difference between PHA-L/vGluT2-positive and PHA-L/vGluT2-negative terminals in the CeM ($p < 0.0001$), and in the Pf ($p < 0.0001$). (*$p<0.05$)

REFERENCES

Bellocchio EE, Hu H, Pohorille A, Chan J, Pickel V, Edwards RH. (1998). The localization of the brain-specific inorganic phosphate transporter suggests a specific presynaptic role in glutamatergic transmission. J. Neurosci. 18**,** 8648-8659.

Boulland JL, Qureshi T, Seal RP, Rafiki A, Gundersen V, Bergersen LH, Fremeau RT Jr, Edwards RH, Storm- Mathisen J, Chaudhry FA. (2004). Expression of the vesicular glutamate transporters during development indicates the widespread corelease of multiple neurotransmitters. J Comp Neurol 480: 264 280

Choi DW, Maulucci-Gedde M, Kriegstein AR. (1987). Glutamate neurotoxicity in cortical cell culture J Neurosci 7: 357 368

De Gois S, Schafer MK, Defamie N, Chen C, Ricci A, Weihe E, Varoqui H, Erickson JD. (2005). Homeostatic scaling of vesicular glutamate and GABA transporter expression in rat neocortical circuits. J Neurosci 25: 7121 7133

Fonnum F. (1984). Glutamate: a neurotransmitter in mammalian brain. J Neurochem 42: 1 11

Fremeau RT Jr, Troyer MD, Pahner I, Nygaard GO, Tran CH, Reimer RJ, Bellocchio EE, Fortin D, Storm- Mathisen J, Edwards RH (2001) The expression of vesicular glutamate transporters defines two classes of excitatory synapse Neuron 31: 247 260

Fremeau RT Jr, Kam K, Qureshi T, Johnson J, Copenhagen DR, Storm-Mathisen J, Chaudhry FA, Nicoll RA, Edwards RH. (2004). Vesicular glutamate transporters 1 and 2 target to functionally distinct synaptic release sites. Science;304(5678):1815-9. Epub. PubMed PMID: 15118123.

Fremeau RT Jr, Burman J, Qureshi T, Tran CH, Proctor J, Johnson J, Zhang H, Sulzer D, Copenhagen DR, Storm- Mathisen J, Reimer RJ, Chaudhry FA, Edwards RH. (2002). The identification of vesicular glutamate transporter 3 suggests novel modes of signaling by glutamate. Proc Natl Acad Sci U S A 99: 14488 14493

Fremeau RT Jr, Troyer MD, Pahner I, Nygaard GO, Tran CH, Reimer RJ, Bellocchio EE, Fortin D, Storm- Mathisen J, Edwards RH (2001) The expression of vesicular glutamate transporters defines two classes of excitatory synapse Neuron 31: 247 260

Fujiyama F, Furuta T, Kaneko T (2001) Immunocytochemical localization of candidates for vesicular glutamate transporters in the rat cerebral cortex J Comp Neurol 435: 379 387

Galvan, A., Kuwajima, M., & Smith, Y. (2006). Glutamate and GABA receptors and transporters in the basal ganglia: What does their subsynaptic localization reveal about their function? *Neuroscience*, *143*(2), 351–375. http://doi.org/10.1016/j.neuroscience.2006.09.019

Gonzalez, L. M., Williamson, I., Piedrahita, J. A., Blikslager, A. T., & Magness, S. T. (2013). Cell Lineage Identification and Stem Cell Culture in a Porcine Model for the Study of Intestinal Epithelial Regeneration. *PLoS ONE, 8*(6), e66465. http://doi.org/10.1371/journal.pone.0066465

Gras C, Herzog E, Bellenchi GC, Bernard V, Ravassard P, Pohl M, Gasnier B, Giros B, El Mestikawy S (2002) A third vesicular glutamate transporter expressed by cholinergic and serotoninergic neurons J Neurosci 22: 5442 5451

Herzog E, Bellenchi GC, Gras C, Bernard V, Ravassard P, Bedet C, Gasnier B, Giros B, El Mestikawy S (2001) The existence of a second vesicular glutamate transporter specifies subpopulations of glutamatergic neurons J Neurosci 21: RC181

Herzog E, Gilchrist J, Gras C, Muzerelle A, Ravassard P, Giros B, Gaspar P, El Mestikawy S (2004) Localization of VGLUT3, the vesicular glutamate transporter type 3, in the rat brain Neuroscience 123: 983 1002

Hur EE, Zaborszky L (2005) Vglut2 afferents to the medial prefrontal and primary somatosensory cortices: a combined retrograde tracing in situ hybridization J Comp Neurol 483: 351 373

Kaneko T, Fujiyama F, Hioki H (2002) Immunohistochemical localization of candidates for vesicular glutamate transporters in the rat brain J Comp Neurol 444: 39 62

Lee RYN, Sawin ER, Chalfie M, Horvitz HR, Avery L. EAT-4, a Homolog of a Mammalian Sodium-Dependent Inorganic Phosphate Cotransporter, Is Necessary for Glutamatergic Neurotransmission in *Caenorhabditis elegans*. *The Journal of neuroscience: the official journal of the Society for Neuroscience*. 1999;19(1):159-167.

Lievens JC, Woodman B, Mahal A, Spasic-Boscovic O, Samuel D, Kerkerian-Le Goff L, Bates GP (2001) Impaired glutamate uptake in the R6 Huntington's disease transgenic mice Neurobiol Dis 8: 807 821

Mathai A, Ma Y, Paré JF, Villalba RM, Wichmann T, Smith Y. (2015). Reduced cortical innervation of the subthalamic nucleus in MPTP-treated parkinsonian monkeys. Brain. 2015 Apr;138(Pt 4):946-62. doi: 10.1093/brain/awv018. PubMed PMID: 25681412.

Maragakis NJ, Rothstein JD (2004) Glutamate transporters: animal models to neurologic disease Neurobiol Dis 15: 461 473

Masliah E (2000) The role of synaptic proteins in Alzheimer's disease Ann N Y Acad Sci 924: 68 75

Matsumoto N, Minamimoto T, Graybiel AM, Kimura M. (2001). Neurons in the thalamic CM-Pf complex supply striatal neurons with information about behaviorally significant sensory events. J Neurophysiol;85(2):960-76. PubMed PMID: 11160526.

Nakamura K, Hioki H, Fujiyama F, Kaneko T (2005) Postnatal changes of vesicular glutamate transporter (VGluT)1 and VGluT2 immunoreactivities and their colocalization in the mouse forebrain J Comp Neurol 492: 263 288

Ni B, Rosteck PR Jr, Nadi NS, Paul SM. (1994). Cloning and expression of a cDNA encoding a brain-specific Na(+)- dependent inorganic phosphate cotransporter. Proc Natl Acad Sci U S A 91: 5607 5611

Persson S, Boulland JL, Aspling M, Larsson M, Fremeau RT Jr, Edwards RH, Storm-Mathisen J, Chaudhry FA, Broman J. (2006). Distribution of vesicular glutamate transporters 1 and 2 in the rat spinal cord, with a note on the spinocervical tract. J Comp Neurol 497: 683 701

Raju DV, Smith Y. (2006). Anterograde axonal tract tracing. Curr Protoc Neurosci;Chapter 1:Unit 1.14. doi: 10.1002/0471142301.ns0114s37. Review. PubMed PMID: 18428632.

Raju DV, Ahern TH, Shah DJ, Wright TM, Standaert DG, Hall RA, Smith Y. (2008). Differential synaptic plasticity of the corticostriatal and thalamostriatal systems in an MPTP-treated monkey model of parkinsonism. Eur J Neurosci; (7):1647-58. doi: 10.1111/j.1460-9568.2008.06136.x. PubMed PMID: 18380666.

Sadikot AF, Parent A, Smith Y, Bolam JP. (1992). Efferent connections of the centromedian and parafascicular thalamic nuclei in the squirrel monkey: a light and electron microscopic study of the thalamostriatal projection in relation to striatal heterogeneity. J Comp Neurol;320(2):228-42. PubMed PMID: 1619051.

Sakata-Haga H, Kanemoto M, Maruyama D, Hoshi K, Mogi K, Narita M, Okado N, Ikeda Y, Nogami H, Fukui Y, Kojima I, Takeda J, Hisano S. (2001). Differential localization and colocalization of two neuron-types of sodium- dependent inorganic phosphate cotransporters in rat forebrain Brain Res 902: 143 155

Sepkuty JP, Cohen AS, Eccles C, Rafiq A, Behar K, Ganel R, Coulter DA, Rothstein JD (2002) A neuronal glutamate transporter contributes to neurotransmitter GABA synthesis and epilepsy J Neurosci 22: 6372 6379

Shyu A-B, Wilkinson MF, van Hoof A. (2008). Messenger RNA regulation: to translate or to degrade. *The EMBO Journal*;27(3):471-481. doi:10.1038/sj.emboj.7601977.

Smith Y, Raju DV, Pare JF, Sidibe M. (2004). The thalamostriatal system: a highly specific network of the basal ganglia circuitry. Trends Neurosci; (9):520-7. Review. PubMed PMID: 15331233.

Smith, Y., Galvan, A., Ellender, T. J., Doig, N., Villalba, R. M., Huerta-Ocampo, I., Bolam, J. P. (2014). The thalamostriatal system in normal and diseased states. *Frontiers in Systems Neuroscience, 8*, 5. http://doi.org/10.3389/fnsys.2014.00005

Takamori S, Rhee JS, Rosenmund C, Jahn R (2000) Identification of a vesicular glutamate transporter that defines a glutamatergic phenotype in neurons Nature 407: 189 194

Unal G, Paré JF, Smith Y, Paré D. (2014). Cortical inputs innervate calbindin-immunoreactive interneurons of the rat basolateral amygdaloid complex. J Comp Neurol;522(8):1915-28. doi: 10.1002/cne.23511. PubMed PMID: 24285470; PubMed Central PMCID: PMC3984626.

Varoqui H, Schafer MK, Zhu H, Weihe E, Erickson JD (2002) Identification of the differentiation-associated Na+/PI transporter as a novel vesicular glutamate transporter expressed in a distinct set of glutamatergic synapses J Neurosci 22: 142 155

Villalba RM, Mathai A and Smith Y (2015) Morphological changes of glutamatergic synapses in animal models of Parkinson's disease. Front. Neuroanat. 9:117. doi: 10.3389/fnana.2015.00117